Magnetically Shielded Miniature Hall Thruster: Design Improvement and Performance Analysis

Ryan W. Conversano[1]
University of California Los Angeles, Los Angeles, CA, 90095, USA

Dan M. Goebel[2], Richard R. Hofer[3], Ioannis G. Mikellides[4], and Ira Katz[5]
Jet Propulsion Laboratory, California Institute of Technology, Pasadena, CA, 91109

and

Richard E. Wirz[6]
University of California Los Angeles, Los Angeles, CA, 90095, USA

ABSTRACT: Magnetic shielding has been shown to dramatically reduce discharge channel wall erosion of high powered Hall thrusters, thereby increasing their useful lifetimes. However, unique challenges exist for developing a low power magnetically shielded Hall thruster. A previously tested 4 cm magnetically shielded miniature Hall thruster demonstrated low performance of its magnetic circuit, resulting in an asymmetric field topology, low thrust, and low efficiency. A 6 cm magnetically shielded Hall thruster was developed to improve upon the 4 cm design. The 6 cm device, which generated a symmetric and fully shielded field topology, was tested at 30 operating conditions ranging from 160 W to nearly 750 W. Visual observation of the plasma and discharge channel during and after operation was used to assess the level of magnetic shielding that was achieved. Hall2De plasma simulations were also used to offer further evidence of magnetic shielding. Thrust stand measurements provided thrust, anode specific impulse, and anode efficiency data at each operating condition. Pole face erosion, which is believed to be associated with the 6 cm thruster's non-optimized magnetic shielding field topology and strength, identify the near-term challenges to resolve before long lifetimes and high efficiencies can be achieved in low power Hall thrusters.

---

[1] PhD Candidate, Dept. of Mechanical and Aerospace Engineering (ryan.w.conversano@jpl.nasa.gov)
[2] Senior Research Scientist, Propulsion, Thermal, and Materials Section (dan.m.goebel@jpl.nasa.gov)
[3] Senior Engineer, Electric Propulsion Group (richard.r.hofer@jpl.nasa.gov)
[4] Principal Engineer, Electric Propulsion Group (ioannis.g.mikellides@jpl.nasa.gov)
[5] Principal Engineer and Group Supervisor, Electric Propulsion Group (ira.katz@jpl.nasa.gov)
[6] Associate Professor, Dept. of Mechanical and Aerospace Engineering (wirz@ucla.edu)

I.   Introduction

Efficient, high ΔV, low power Hall thrusters are an enabling technology for a variety of NASA missions. Deep space and near Earth missions, especially those using sub-500 kg spacecraft, would be made possible due to these thrusters' combined advantages of high specific impulse and high thrust-to-power ratios at a reduced scale [1]. A major challenge in developing such a device is maintaining a high level of performance while achieving sufficient operational life, which is limited by several factors.

The primary life-limiting mechanisms for conventional Hall thrusters are erosion of the discharge channel walls due to ion bombardment and thermal heating due to high-energy electron power loss to the channel. These effects reduce a thruster's performance during operation and yield a reduction in the thruster's useful life through the erosion and overheating of the discharge channel and magnetic circuit components. More details on these mechanisms are presented in the literature [2–10]. The inherently larger surface-to-volume ratio of low power Hall thrusters magnifies the effects of ion bombardment erosion and electron heating. While the erosion rates of conventionally sized and miniature Hall thrusters may be comparable, shorter operational lifetimes are always observed in miniature devices due to their reduced channel wall thickness. Note that Hall thrusters of all power levels may operate long after the discharge channel walls erode with only a minor impact on performance, suggesting that the complete erosion of the discharge channel walls and exposure of the pole pieces to the plasma may not be sufficient to characterize the total operational lifetime of a Hall thruster [11].

While they deliver favorable performance, operational lifetimes of miniature Hall thrusters are generally low, ranging from tens of minutes to hundreds of hours with few devices demonstrating lifetimes beyond 1,000 hours [12–17]. The BHT-200 employs a 30 mm discharge channel diameter and nominally operates at 200 W. It is capable of a maximum thrust of 12.8 mN at a specific impulse of 1390 s and an anode efficiency of 44% (nominally 11.4 mN, 1570 s, and 42%); however, failures of the discharge channel components have been observed after approximately 1,300 h with tests continuing to more than 1,700 h [12,18–21]. The SPT-30, another 30 mm Hall thruster operating at approximately 200 W, produces 11.3 mN of thrust at a specific impulse of 1170 s and an anode efficiency of 32%; this thruster also demonstrates a relatively limited operational life of approximately 600 h [13]. Slightly higher power Hall thrusters (corresponding to an increase in channel outer diameter) include the SPT-50 and SPT-70. The SPT-50 is a 50 mm Hall thruster with a nominal power of 350 W. It has a demonstrated thrust and specific impulse of 20 mN and 1100 s, respectively, at an anode efficiency of 35% and has a useful life of approximately 1,000 hours [2,14,22]. The SPT-70, with a 70 mm channel outer diameter, operates nominally at 600 - 700 W and produces 40 mN of thrust with a specific impulse of 1500 s at an anode efficiency of 45% [2,22,23]; an operational lifetime in excess of 3,000 hours has been demonstrated [15].

Magnetic shielding significantly reduces the above life limiting factors through careful design of a Hall thruster's magnetic circuit, potentially resulting in dramatically increased operational lifetimes. Magnetic shielding is achieved through a unique field topology that exploits two key features of Hall thruster behavior: the isothermality of magnetic field lines and magnetic force line equipotentialization [24–27]. The field lines passing nearest to but not intersecting the discharge channel walls penetrate deep into the channel and capture cold (~5 eV) electrons from the anode region. Field line isothermality allows these lines, populated by cold electrons, to maintain a low average electron temperature along the discharge channel walls. This leads to the near equipotentialization of the lines of force near the walls, maintaining a plasma potential close to that of the discharge voltage, and a reduction of the plasma sheath potential drop along the walls. These effects combine to significantly reduce the kinetic energy gained by ions that pass through the wall sheath and impact the channel walls, thereby nearly eliminating ion-bombardment erosion of and high-energy electron power deposition to the channel. The concept of magnetic shielding has been successfully demonstrated on multiple high power Hall thrusters and is well understood [24–27].

The ultimate goal of this investigation is to develop a fully shielded low power Hall thruster that demonstrates significantly increased operational lifetimes compared to existing low power Hall thrusters and to analyze the effects of the life-extending mechanisms on the thruster's performance. The primary objectives for this portion of the investigation were as follows:

1) Determine the cause of the asymmetric, partially shielded magnetic field topology and low performance of the MaSMi Hall thruster.
2) Develop a new version of the MaSMi Hall thruster with a fully shielded field topology.
3) Demonstrate significantly increased lifetimes of the MaSMi Hall thruster resulting from nearly eliminating wall erosion.
4) Examine any changes in performance resulting from the reduction of plasma-wall interactions and high energy electron power losses.

In this paper, experimental and computational results from a fully magnetically shielded low power Hall thruster are presented. Section II begins with a review of the work completed using the original magnetically shielded miniature (MaSMi) Hall thruster (herein called the MaSMi-40 based on its ~40 mm discharge channel outer diameter). Section III presents the design considerations used to develop the MaSMi-60, an updated version of the original MaSMi Hall thruster with a ~60 mm discharge channel outer diameter. The experimental facility and setup are discussed in Section IV. Experimental results and discussion are presented in Section V. Section VI shows the initial computational results from Hall2De models of the plasma inside and local to the discharge channel. Lastly, suggested future work and concluding remarks are presented in Sections VII and VIII, respectively.

II.   Previous Work

The MaSMi-40 Hall thruster was developed in a collaborative effort between the University of California, Los Angeles (UCLA) and NASA's Jet Propulsion Laboratory (JPL). This device, which was designed to operate between 200 - 400 W, was intended to demonstrate that a magnetically shielded field topology applied to a low power Hall thruster would yield increased operational life while possibly improving the thruster's performance. Details on the design and supporting equipment of the thruster can be found in the previous papers from this investigation [8–10].
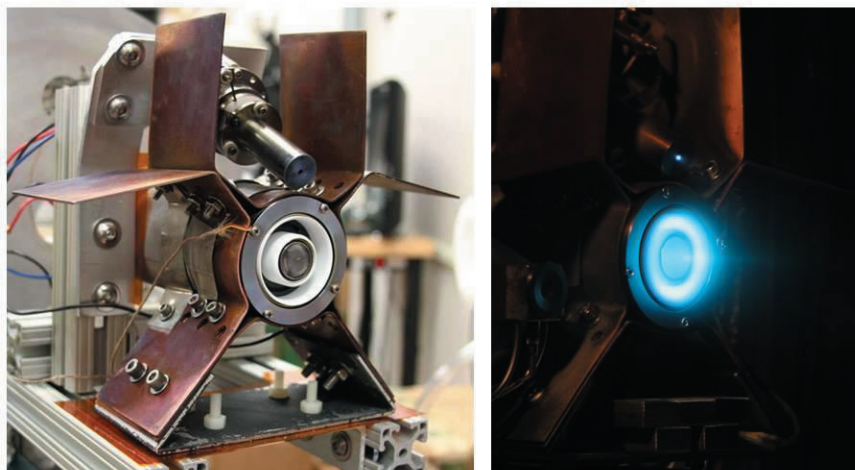

Figure. 1. The MaSMi-40 Hall thruster before and during operation at 330 W.

The MaSMi-40 Hall thruster, shown before and during operation in Figure 1, has been operated at two vacuum facilities: the UCLA Electric Propulsion Test Facility and the JPL High Bay facility. MaSMi-40 testing at UCLA focused on the nominal operating power of 325 - 330 W, while testing at the JPL facility spanned a range of power levels, from 130 - 640 W. A full diagnostic suite at JPL, including direct thrust measurements from a thrust stand, allowed for a more complete characterization of the thruster's performance at 330 W, resulting in a thrust of approximately 13 mN at an anode efficiency of approximately 24% [10]. The thrust produced by the MaSMi-40 over the full operating power range was measured from less than 5 mN to over 20 mN [10]. During testing, the thruster's plasma beam was observed to have a significantly different structure and behavior at the two facilities. Multiple operation modes were observed, each corresponding to different performance levels and closely related to the thruster's operating temperature [10]. Identification of at least two unique modes at the JPL facility and a single mode at UCLA were confirmed with plume measurements [10].

A thorough investigation of the MaSMi-40's magnetic field topology revealed significant asymmetry in the field structure: the outer discharge channel wall was well shielded while the inner channel wall was, at best, partially shielded in certain operating conditions. The poor magnetic shielding of the MaSMi-40 was the result of both a lack of understanding of the scaling limits of magnetic shielding to low power Hall thrusters and convergence issues in the computational design tools used to design the MaSMi-40 thruster that were discovered after fabrication of the device. An explanation of the problems discovered with the magnetic circuit design tools, along with a thorough sensitivity analysis and validation of an updated version of the software, has been published in detail in a companion paper [28].

III. Overview of the MaSMi-60

A. Geometry

The design for the MaSMi-60's magnetic circuit was completed using the process and key geometry considerations discussed in [8,9,28]. The MaSMi-60's low power capabilities were maintained by keeping the discharge channel exit area as small as possible while allowing a sufficient channel width to achieve the desirable magnetic field topology across the channel. The MaSMi-60's discharge channel has a b/d_m ratio of 0.157, which is notably lower than the established b/d_m trends for low power Hall thrusters [8,9]. However, this value is very similar to the b/d_m ratios used in moderate- to high-power Hall thrusters, especially those aiming to achieve high specific impulse [29]. A variable-placement anode, using the same two-chamber design from the MaSMi-40, allows for a range of discharge channel lengths up to twice the channel width.

B. Magnetic Field

Near perfect agreement was observed between the field topologies predicted by the validated magnetic fields software and the measured field; the predicted and measured peak radial field strength along the channel centerline ($B_{r,max}$) matched to within 1%. A symmetric topology was measured to remain constant over a large range of $B_{r,max}$ (<150 G to <250 G). At a $B_{r,max}$ of approximately 200 G, the magnetic circuit shows no signs of saturation onset. The presence of moderate saturation is predicted as field strengths exceed 225 G; however, the level of saturation is significantly lower than that of the MaSMi-40 at its nominal coil conditions, which yielded an asymmetric topology with a measured $B_{r,max}$ of less than 150 G.

C. Thermal Considerations

The thermal overheating observed during operation of the MaSMi-40 suggested that a significantly improved thermal design was necessary for the MaSMi-60, leading to the development of a more sophisticated thermal model. Details on this model can be found in [28]. The improved thermal model was validated against temperature measurements taken for the MaSMi-40 and then applied to the MaSMi-60. At an assumed discharge power of 450 W, approximately 170 W of plasma heating of the discharge channel was predicted by the power deposition model presented in [8,9]. Using this value, along with conservative estimates of 55 W and 22 W for the inner and outer magnet coils (based on the MaSMi-40 coil conditions), respectively, a body temperature of approximately 450°C was predicted for the MaSMi-60. This result, which represents a worst case scenario as it assumes no thermal radiator and high magnet powers, suggests a significant improvement in thermal design over the MaSMi-40.

In an effort to further ensure that no thermal problems would inhibit the performance of the MaSMi-60, the thruster was mounted to a radiator consisting of a square copper plate with notch removed to allow clearance for the cathode. The overall profile of the radiator was selected to simulate the thruster mounting region of a spacecraft, with the maximum dimensions only as big as necessary to accommodate the hollow cathode used in these experiments. The copper radiator was heat treated with an asetylene torch to achieve a dark surface color, yielding an

Figure 2. MaSMi-60 mounted to the High Bay Facility thrust stand via the thermal radiator.

increased emissivity. While the radiator was used to mount the thruster to the thrust stand, multiple layers of Mica were used between each metal-metal interface to effectively thermally isolate the thruster from the water-cooled thrust stand. An image of the thruster mounted to the radiator and interfaced to the thrust stand is presented in Figure 2.
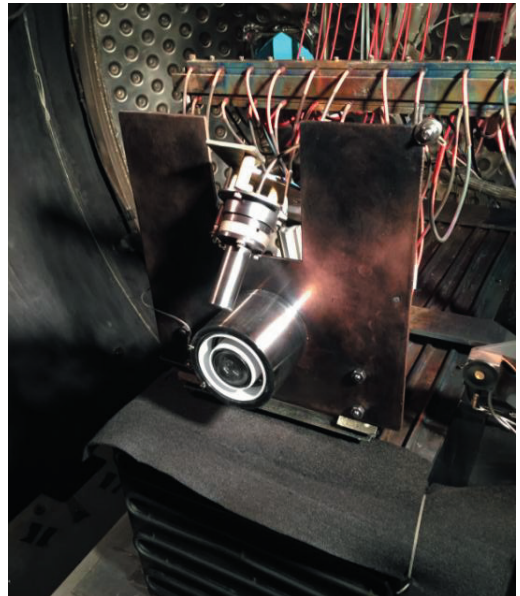
IV. Experiment Configuration

A. Vacuum Facility and Supporting Equipment

Experimental testing was conducted at the High-Bay vacuum facility at the Jet Propulsion Laboratory. The High-Bay facility utilizes a cylindrical vacuum chamber measuring 2.6 m in diameter and 5.2 m long. All internal surfaces of the chamber with line-of-sight to the thruster's discharge channel are covered with either graphite panels or other carbon material. Three cryogenic pumps are operated in parallel for a combined xenon pumping speed of approximately 40,000 l/s. The chamber pressure is monitored by two ionization gauges, both calibrated for xenon. The first gauge is located on the thruster exit plane approximately 1 m from the thruster and is used as the primary indication of chamber pressure. The second gauge, used to confirm pressure readings from the first gauge, is mounted along the chamber wall just downstream of the thruster exit plane. For these experiments, the base pressure of the system was less than 1.5×10^{-7} Torr, corrected for xenon. During operation with xenon flow of approximately 30 sccm, the chamber pressure remained below 1.5×10^{-5} Torr. A propellant flow bypass, regulated by a hand-operated needle valve, is incorporated into the flow system (flow outlet located approximately 2 m downstream of and oriented away from thruster face) to increase the facility background pressure if desired.

Commercially available power supplies and propellant flow controllers were used for all experiments. Thruster discharge, cathode heater, and cathode keeper power was supplied by Sorensen DLM-series power supplies while the coil magnets were powered by Power Ten supplies. Research grade xenon was supplied to the thruster and cathode by Apex mass flow controllers via stainless steel lines. Both controllers were calibrated prior to testing and were digitally controlled to an accuracy of ± 1% of the set point. A BaO-W cathode based on the ISS plasma contactor cathode and NSTAR ion thruster cathode was utilized for this investigation. The cathode was mounted at a 45° angle with respect to the thruster axis with the cathode orifice approximately one discharge channel outer diameter above the thruster centerline and in plane with the discharge channel exit.

B. Diagnostics

The JPL High-Bay vacuum facility employs eight thruster and plasma diagnostics, including a thrust stand, discharge plasma probes, temperature probes, and carbon back-sputter measurement probes. Of these diagnostics, those utilized for this investigation are as follows:

1) Thrust stand: directly measures thrust, from which specific impulse and efficiency can be calculated. The thrust stand demonstrated a minimum thrust resolution of approximately +/- 0.1 mN with an uncertainty of approximately +/- 1 mN, validated against a BHT-200 operating at nominal conditions.
2) Current probe: measures discharge current oscillations. The current probe was mounted on the thruster's anode power cable fed to a Tektronix oscilloscope on the plasma side of the discharge filter.
3) Thermocouples: monitor temperature during thruster operation. K-type thermocouples were mounted to the thruster's front outer pole and back plate at multiple locations to determine local temperatures as well as the axial and radial temperature gradients across the thruster.

While only thrust stand, discharge current oscillation, and temperature measurements were taken for this portion of the MaSMi-60 performance investigation, a full plasma beam characterization will be performed in the near future to be published thereafter.

V. Experimental Results and Discussion

A. Operating Conditions

A summary of the operating conditions used for thrust stand measurements is presented in Table 1. The test matrix shows the nominal power achieved as a function of discharge voltage and anode propellant flow rate. Testing of the MaSMi-60 Hall thruster was conducted at a range of discharge voltages from 200 V to 400 V in increments of 50 V. At each of the five discharge voltages, the propellant flow rate was varied from 12 sccm to 28 sccm in increments of 2 sccm; the flow rate was increased until 28 sccm was achieved with stable thruster operation or until the thruster demonstrated unfavorable behaviors, such as localized wall heating (these conditions are marked with an "X" in Table 1). This matrix of voltages and flow rates at the nominal operating point for each condition yielded a range of discharge powers from 160 W to nearly 750 W. A total operation time in excess of 55 hours was logged during this testing campaign.

It should be noted that the nominal operating point, defined as the minimum discharge current as a function of $B_{r,max}$ for a given discharge voltage and propellant flow rate, was not necessarily the absolute minimum discharge current but rather the minimum current attainable with the available magnetic field settings. This is discussed further in Section VI.C.

Table 1. Operating conditions for the MaSMi-60 Hall thruster during thrust stand measurements, summarizing the nominal power achieved as a function of discharge voltage and anode flow rate.

		Discharge Voltage (V)				
		200	**250**	**300**	**350**	**400**
Anode Flow Rate (sccm)	**12**	160 W	205 W	243 W	291 W	344 W
	14	200 W	255 W	309 W	368 W	420 W
	16	242 W	308 W	378 W	487 W	596 W
	18	290 W	363 W	453 W	560 W	X
	20	346 W	448 W	549 W	X	X
	22	436 W	548 W	720 W	X	X
	24	502 W	643 W	X	X	X
	26	564 W	745 W	X	X	X
	28	628 W	X	X	X	X

The cathode flow rate was held to approximately 7-8% of the anode flow rate, but was never supplied with less than 1 sccm. The thruster was operated both with and without an applied keeper current of 2 A, resulting in no observed sensitivities of the thruster operation to the application of keeper current. The cathode-ground potential remained between -8 V and -20 V, depending on the specific operating condition. During all tests, the thruster was allowed to float from chamber ground and the discharge channel length (based on anode placement) was set to twice the discharge channel width. Temperatures measured at the front outer pole and near the center core at the back pole remained below 250°C and 200°C, respectively, for all tests; the temperature gradient along the radius of the back pole remained below 30°C.

B. Magnetic Shielding

To assess the effectiveness of magnetic shielding in the MaSMi-60, a visual analysis of the plasma discharge during operation and an examination of the discharge channel before and after operation were conducted. An image of the plasma discharge of MaSMi-60 is presented in Figure 3; the camera settings were optimized to view the highest density plasma region in the discharge channel. Large gaps between the plasma and the discharge channel walls are easily identified, suggesting that both the inner and outer channel walls are successfully shielded [27].

Figure 3. Operation of the MaSMi-60 at 250 V and 335 W showing evidence of successful magnetic shielding through a clear offset of the plasma from the inner and outer discharge channel walls.

Figure 4 shows an image of the discharge channel before and after thruster operation. The clean white BN channel was uniformly coated in a layer of carbon, back-sputtered from the graphite panels along the walls of the vacuum chamber. Like the H6MS, these observations are visual evidence of a fully shielded magnetic field topology [6,27].

Figure 4. Comparison of the MaSMi-60's discharge channel and pole faces before and after ~ 20 hours of operation. Note the uniform layer of carbon deposited on the inner and outer cannel walls, suggesting the presence of magnetic shielding, and the level of front inner and outer pole face erosion.

Significant erosion of both the inner and outer pole pieces was observed throughout testing of the MaSMi-60. The images of the MaSMi-60 in Figure 4 show the level of the pole face erosion after approximately 20 hours of operation. This feature is known to affect high power magnetically shielded Hall thrusters and is believed to be the result of the non-optimized magnetic shielding field topology. Specifically, though the MaSMi-60 achieves symmetric shielding of the inner and outer walls (compared to the MaSMi-40), it also imposes a topology around the chamfered regions of the discharge channel with exceedingly high field curvature (see Sec. VI), much higher than in the designs of this thrusters' high-power counterparts (termed "over-shielded"). This, in turn, may lead to higher angular divergence of beam ions and higher pole erosion. The stability of the thruster may also be jeopardized, leading to higher than desired plasma oscillations which could enhance erosion. These and other possible physical mechanism(s) of ion bombardment of the pole faces are under investigation [30].

C. Performance Measurements
1) Thrust
Thrust stand measurements were taken at the 30 operating conditions presented in Table 1. The thrust produced as a function of discharge power for each operating discharge voltage is shown in Figure 5. Increases in discharge power yielded proportional increases in thrust, generating highly linear trends for each discharge voltage. Thrust values ranging from 8 mN to over 33 mN were observed across all operating points, demonstrating the favorable throttling range of the MaSMi-60.
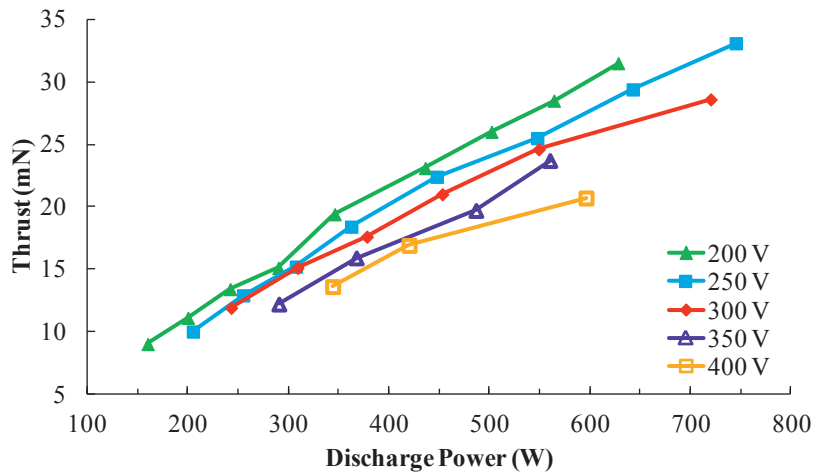
Figure 5. Thrust as a function of discharge power for the MaSMi-60.

2) Anode Specific Impulse

The anode specific impulse (I_{sp}) as a function of discharge power for the MaSMi-60 is shown in Figure 6. All curves followed the expected trends of increasing I_{sp} with both discharge voltage and discharge power. Specific impulse values of between 730 s and 1370 s were observed across the full range of operating conditions. These results suggest that the MaSMi-60 achieves slightly lower I_{sp} values at a given power level than conventional low power Hall thrusters of a similar-scale. This is likely due to the plasma being forced far downstream of the discharge channel exit by the over-shielded magnetic field topology, causing a poor propellant utilization fraction and an associated reduction in specific impulse.
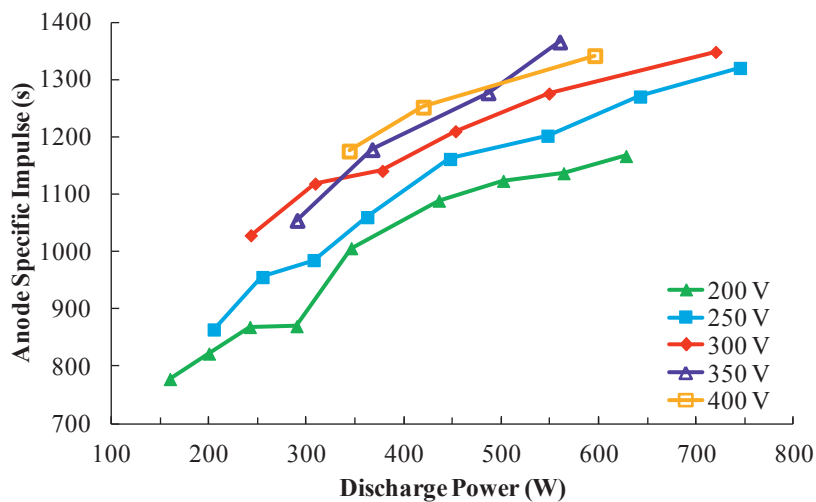

Figure 6. Anode specific impulse as a function of discharge power for the MaSMi-60.

3) Anode Efficiency

The MaSMi-60's anode efficiency as a function of discharge power is presented in Figure 7. In general, all operating conditions yielded increased efficiency as the discharge power was increased. In every case except the 400 V conditions, however, there appeared to be an efficiency ceiling between 28% and 29% where the thruster

would remain as discharge power was increased. This efficiency ceiling is likely caused, at least in part, by the over-shielded topology, which forces the plasma far downstream of the discharge channel reducing plasma confinement and focusing while enabling increased neutral leakage.
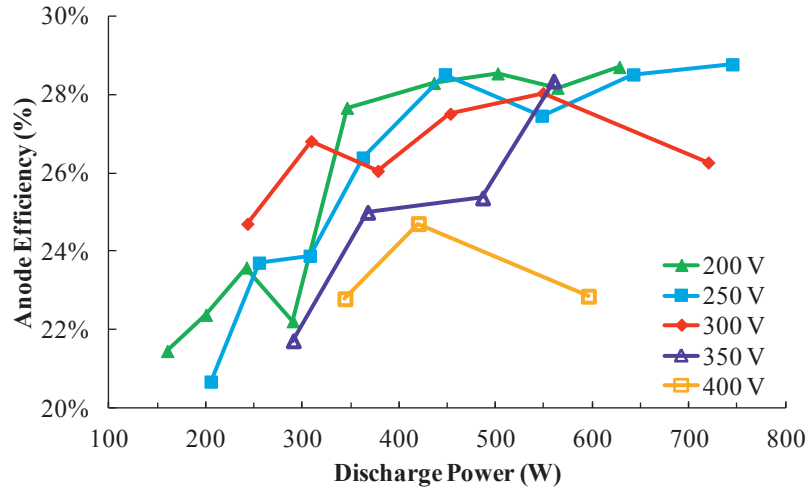

Figure 7. Anode efficiency as a function of discharge power for the MaSMi-60.

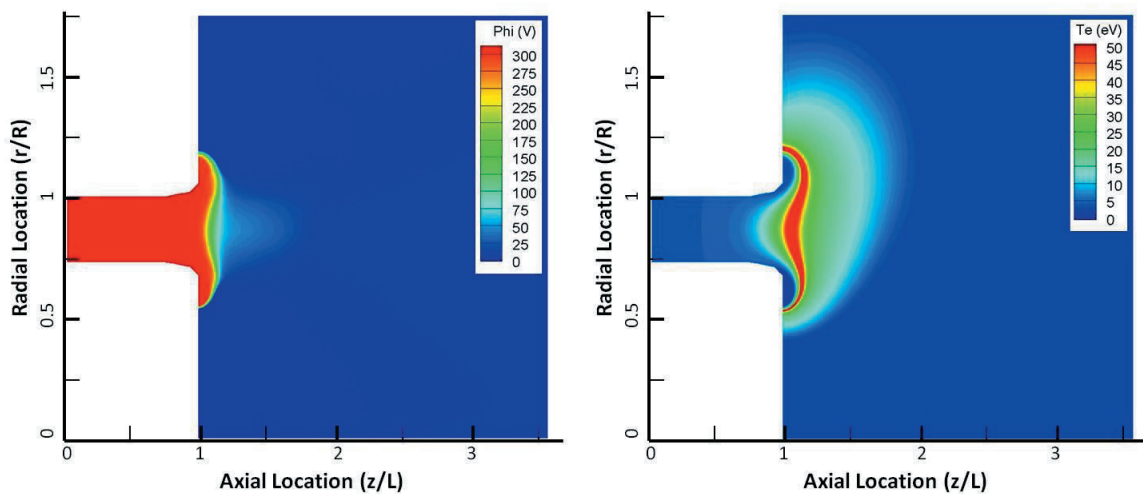## VI. Preliminary Computational Results

Figure 8. Plasma potential (left) and electron temperature (right) Hall2De simulations of the MaSMi-60 operating at a discharge voltage of 300 V and a discharge current of 1.4 A in terms of the discharge channel length (L) and outer radius (R).

Simulations of the plasma inside and local to the discharge channel were generated using Hall2De, a two-dimensional solver for the governing conservation equations of the partially ionized gases in Hall thrusters using a magnetic field aligned computational grid [31,32]. While this computational investigation is ongoing, initial results for a sample operating condition of 300 V discharge voltage and 1.4 A discharge current are presented. Contour plots of the plasma potential and electron temperature are shown on the left and right cells of Figure 8, respectively.

The simulations show the equipotentialization of the field lines through the near-constant plasma potential along the length of the discharge channel. Additionally, hot electrons are confined downstream of the discharge

channel while cold electrons (nearly the same temperature as those adjacent to the anode) are held near the channel walls. It has been shown that these features combine to significantly reduce ion acceleration towards the plasma sheath, the magnitude of the channel wall sheath potential, and therefore the kinetic energy of ions that strike the walls; this is the basis of magnetic shielding [24–27]. While more work is necessary to validate these results, the early simulations suggest that the MaSMi-60 demonstrates the basic tenants of magnetic shielding and provide evidence in support of the above claims of magnetic shielding based on visual observations of the plasma and discharge channel (discussed in Section V.B). The results also underscore the need for further optimization of the magnetic field, which at present imposes an exceedingly curved topology of the lines around the chamfered region and drives acceleration of ions to occur far downstream of the channel exit. Though not yet confirmed, both these effects could be main contributors to the observed pole erosion.

VII. Future Work

A full characterization of the MaSMi-60's plasma beam will be carried out using the existing plasma and beam diagnostics at the JPL High Bay vacuum facility. These measurements will be compared to the thrust stand results to achieve a clear understanding of the operation and behavior of the MaSMi-60. Carbon back-sputter measurements will be taken at several of the MaSMi-60's more promising operating conditions (i.e. those that yielded the best combinations of thrust, efficiency, and discharge stability) using a QCM. These data can be related to discharge channel erosion rates, and therefore useful life, for magnetically shielded Hall thrusters based on theory presented in the literature [6,27]. The Hall2De computational effort will be continued to offer further validation of magnetic shielding and to describe any unique plasma behaviors of the MaSMi-60 that may be different than either conventional low power Hall thrusters or high power magnetically shielded devices. Following the full characterization of the MaSMi-60, methods to reduce the over-shielding will be examined in an effort to reduce pole face erosion, maintain operational lifetime, and improve performance.

VIII. Conclusion

This investigation successfully demonstrated the applicability of a fully magnetically shielded field topology to low power Hall thrusters. Analyzing the experimental and computational data from the MaSMi-40 Hall thruster enabled the development of the MaSMi-60. A fully shielded magnetic field topology was generated by the MaSMi-60 both in ambient conditions, confirmed through magnetic field mapping, and during operation, based on visual observations of the plasma offset from the discharge channel and carbon deposition patterns on the channel walls. Initial plasma simulation results from Hall2De offered further evidence that the MaSMi-60 was magnetically shielded. The MaSMi-60 also showed clear evidence of pole face erosion after approximately 20 hours of operation at rates that appear to be much higher than those observed in high-power Hall thrusters, suggesting the need for further optimization of the magnetic shielding topology and investigation into mitigation techniques (if needed). Thrust stand measurements taken at 30 operating conditions ranging from 160 W to nearly 750 W of discharge power yielded a throttling range of 8 mN to 33 mN of thrust and 730 s to 1370 s of anode specific impulse at anode efficiencies ranging from 21% to 29%. While the efficiency is equal to or slightly below that of similar-sized unshielded low power Hall thrusters, the MaSMi-60 demonstrated strong performance with a large throttling range and evidence of significantly increased lifetimes associated with the lack of discharge channel wall erosion.

References

[1]   Conversano, R. W., Arora, N., Goebel, D. M., and Wirz, R. E., "Preliminary Mission Capabilities Assessment of a Magnetically Shielded Miniature Hall Thruster," IAC-14.C4.4.4, *65th International Astronaturical Congress*, Toronto, Canada, Oct. 2014.
[2]   Goebel, D. and Katz, I., *Fundamentals of Electric Propulsion: Ion and Hall Thrusters*. Hoboken, NJ: John Wiley & Sons, Inc., 2008.

[3] Ahedo, E. and Gallardo, J. M., "Scaling Down Hall Thrusters," IEPC-2003-104, *28th International Electric Propulsion Conference*, Toulouse, France, Mar. 2003.

[4] Warner, N. Z., "Theoretical and Experimental Investigation of Hall Thruster Miniaturization," Massachusetts Institute of Technology, 2007.

[5] Mikellides, I. G., Katz, I., and Hofer, R. R., "Design of a Laboratory Hall Thruster with Magnetically Shielded Channel Walls , Phase I : Numerical Simulations," AIAA-2011-5809, *47th AIAA/ASME/SAE/ASEE Joint Propulsion Conference*, San Diego, CA, Jul. 2011.

[6] Hofer, R. R., Goebel, D. M., Mikellides, I. G., and Katz, I., "Design of a Laboratory Hall Thruster with Magnetically Shielded Channel Walls , Phase II : Experiments," AIAA-2011-5809, *48th AIAA/ASME/SAE/ASEE Joint Propulsion Conference*, Atlanta, GA, Jul. 2012.

[7] Mikellides, I. G., Katz, I., Hofer, R. R., and Goebel, D. M., "Design of a Laboratory Hall Thruster with Magnetically Shielded Channel Walls, Phase III: Comparison of Theory with Experiment," AIAA-2012-3789, *48th AIAA/ASME/SAE/ASEE Joint Propulsion Conference*, Atlanta, GA, Jul. 2012.

[8] Conversano, R. W., Goebel, D. M., Hofer, R. R., Matlock, T. S., and Wirz, R. E., "Magnetically Shielded Miniature Hall Thruster : Development and Initial Testing," IEPC-2013-201, *33rd International Electric Propulsion Conference*, Washington D.C., Oct. 2013.

[9] Conversano, R. W., Goebel, D. M., Hofer, R. R., Matlock, T. S., and Wirz, R. E., "Development and Initial Testing of a Magnetically Shielded Miniature Hall Thruster," *IEEE Trans. Plasma Sci.*, vol. 43, no. 1 (2014).

[10] Conversano, R. W., Goebel, D. M., Mikellides, I. G., Hofer, R. R., Matlock, T. S., and Wirz, R. E., "Magnetically Shielded Miniature Hall Thruster: Performance Assessment and Status Update," AIAA-2014-3896, *50th AIAA/ASME/SAE/ASEE Joint Propulsion Conference*, Cleveland, OH, Jul. 2014.

[11] Hofer, R. R., Mikellides, I. G., Katz, I., and Goebel, D. M., "BPT-4000 Hall thruster discharge chamber erosion model comparison with qualification life test data," *30th International Electric Propulsion Conference*, Florence, Italy, Sep. 2007.

[12] Cheng, S. and Martinez-Sanchez, M., "Hybrid Particle-in-Cell Erosion Modeling of Two Hall Thrusters," *J. Propuls. Power*, vol. 24, no. 5, pp. 987–998 (2008).

[13] Jacobson, T. and Jankovsky, R., "Test Results of a 200W Class Hall Thruster," AIAA-98-3792, *34th AIAA Joint Propulsion Confernece*, Cleveland, OH, Jul. 1998.

[14] Manzella, D., Oleson, S., Sankovic, J., Hagg, T., Semenkin, A., and Kim, V., "Evaluation of Low Power Hall Thruster Propulsion," AIAA-96-2736, *32nd AIAA/ASME/SAE/ASEE Joint Propulsion Conference*, Lake Buena Vista, FL, Jul. 1996.

[15] Kim, V., Kozubsky, K., Murashko, V. M., and Semenkin, A., "History of the Hall Thrusters Development in USSR," IEPC-2007-142, *30th International Electric Propulsion Conference*, Florence, Italy, Sep. 2007.

[16] Ito, T., Gascon, N., Crawford, W. S., and Cappelli, M. A., "Further Development of a Micro Hall Thruster," AIAA-2006-4495, *42nd AIAA/ASME/SAE/ASEE Joint Propulsion Conference*, Sacramento, CA, Jul. 2006.

[17] Ito, T., Gascon, N., Crawford, W. S., and Cappelli, M. a., "Experimental Characterization of a Micro-Hall Thruster," *J. Propuls. Power*, vol. 23, no. 5, pp. 1068–1074 (2007).

[18] Hruby, V., Monheiser, J., Pote, B., Kolencik, J., Freeman, C., and Rostler, P., "Development of Low Power Hall Thrusters," AIAA-99-3534, *30th Plasmadynamics and Lasers Conference*, Norfolk, VA, Jul. 1999.

[19] Smirnov, A., Raitses, Y., and Fisch, N. J., "Parametric investigation of miniaturized cylindrical and annular Hall thrusters," *J. Appl. Phys.*, vol. 92, no. 10, p. 5673 (2002).

[20] Hargus, W. A. and Charles, C. S., "Near Exit Plane Velocity Field of a 200 W Hall Thruster," AIAA-2003-5154, *39th AIAA/ASME/SAE/ASEE Joint Propulsion Conference*, Huntsville, AL, Jul. 2003.

[21] Beal, B., Gallimore, A., and Hargus, W. A., "Preliminary Plume Characterization of a Low-Power Hall Thruster Cluster," AIAA-2002-4251, *38th AIAA/ASEE/SAE/ASME Joint Propulsion Confernece*, Indianapolis, ID, Jul. 2002.

[22] Kim, V., Popov, G., Arkhipov, B., Murashko, V., Gorshkov, O., Koroteyev, A., Garkusha, V., Semenkin, A., and Tverdokhlebov, S., "Electric Propulsion Activity in Russia," IEPC-01-05, *27th International Electric Propulsion Conference*, Pasadena, CA, Oct. 2001.

[23] Murashko, V. M., Koryakin, A. I., Nesterenko, A. N., Olotin, S. V, Oranskiy, A. I., Loyan, A. V, Koshelev, M. M., Bilokon, V. I., and Nesterenko, S. Y., "Russian Flight Hall Thrusters SPT-70 & SPT-100 After Cathode Change Start During 20-25 ms," IEPC-2007-62, *30th International Electric Propulsion Conference*, Florence, Italy, 2007.

[24] Mikellides, I. G., Katz, I., Hofer, R. R., Goebel, D. M., de Grys, K., and Mathers, A., "Magnetic shielding of the channel walls in a Hall plasma accelerator," *Phys. Plasmas*, vol. 18, no. 033501 (2011).

[25]   Mikellides, I. G., Katz, I., Hofer, R. R., and Goebel, D. M., "Magnetic shielding of walls from the unmagnetized ion beam in a Hall thruster," *Appl. Phys. Lett.*, vol. 102, no. 023509 (2013).

[26]   Mikellides, I. G., Katz, I., Hofer, R. R., and Goebel, D. M., "Magnetic shielding of a laboratory Hall thruster. I. Theory and validation," *J. Appl. Phys.*, vol. 115, no. 043303 (2014).

[27]   Hofer, R. R., Goebel, D. M., Mikellides, I. G., and Katz, I., "Magnetic shielding of a laboratory Hall thruster. II. Experiments," *J. Appl. Phys.*, vol. 115, no. 043303 (2014).

[28]   Conversano, R. W., Goebel, D. M., Hofer, R. R., Mikellides, I. G., Katz, I., and Wirz, R. E., "Development and Validation Overview for the Design of Low Power Magnetically Shielded Hall Thrusters," *62nd JANNAF Propulsion Meeting*, Nashville, TN, Jun. 2015.

[29]   Hofer, R. R., "Development and Characterization of High-Efficiency, High-Specific Impulse Xenon Hall Thrusters," University of Michigan, 2004.

[30]   Goebel, D. M., Jorns, B. a., Hofer, R. R., Mikellides, I. G., and Katz, I., "Pole-piece Interactions with the Plasma in a Magnetically Shielded Hall Thruster," AIAA 2014-3899, *50th AIAA/ASME/SAE/ASEE Joint Propulsion Conference*, Cleveland, OH.

[31]   Mikellides, I. G. and Katz, I., "Numerical simulations of Hall-effect plasma accelerators on a magnetic-field-aligned mesh," *Phys. Rev. E - Stat. Nonlinear, Soft Matter Phys.*, vol. 86, no. 4 (2012).

[32]   Katz, I. and Mikellides, I. G., "Neutral gas free molecular flow algorithm including ionization and walls for use in plasma simulations," *J. Comput. Phys.*, vol. 230, no. 4, pp. 1454–1464 (2011).